Zeerijp-3A in-situ Strain Analysis

Shell and NAM BV

Pepijn Kole

Datum February 2022

Editors Rob van Eijs and Onno van der Wal

General Introduction

Reservoir compaction is an important factor for subsidence and has therefore been studied since production from the Groningen field commenced. Most compaction monitoring relies on (indirect) measurements of subsidence through optical levelling surveys, GNSS and InSAR. Compaction is then derived either through direct inversion or through compaction models calibrated to these subsidence measurements and/or compaction measurements on core samples.

In Groningen also in-situ measurements of compaction in the reservoir have been taken by logging the relative movement of gamma-ray markers placed in monitoring wells since 1982 (Ref. 1 and 2). In 2015 a fibre-optic cable was installed in well ZRP-3. This allows real-time continuous in-situ monitoring of compaction (Ref. 3).

As reservoir compaction is also an important input into the seismological model, the studies into seismicity in the Groningen gas field have led to an intensified interest in compaction. In 2015, the existing methods as well as a newly developed method to analyse in-situ measurements of compaction in the monitoring wells were reviewed (Ref. 1). This was followed by a more detailed review (Ref. 2) of the in-situ compaction data using gamma ray marker surveys carried out since 2015. The review focussed on the uncertainties in the compaction measurements and whether these are sufficiently accurate to monitor reservoir compaction at the desired depth and time scales.

Compaction can also be measured with the new technology of fibre-optic cables. A glass-fibre cable was installed over the reservoir section of the Zeerijp-3 monitoring well. A year after taking this in-situ compaction measurement system into operation a report describing the first year of experience with this new technology was published (Ref. 3).

The experience in measuring compaction using this system over the first four years of operation was reported in February 2020 (Ref. 4). The acquired dataset is discussed with attention to a number of significant events taking place in these four year, a coiled tubing clean out (CTCO) of the monitoring well, an earthquake of magnitude 3.4 occurring less than 1.5 km from the well, an upgrade of DSS interrogator module, and multiple periods of active geophone operation.

The current report extends the analysis until 31st December 2021. Special attention is given to potential compaction changes during a swarm of earthquakes at approximately 1 km from the well between 4th and 6th October 2021 (Ref. 5 and 6).

An almost continuous compaction dataset has been acquired from 2015 when the Zeerijp-3A well was taken in operation until 31st December 2021. This data set has been made available by NAM through EPOS (European Plate Observatory System). The continuous acquisition of in-situ compaction measurements in the Zeerijp-3A well is carried out as part of the monitoring of the Groningen field.

Reference

1. In-situ compaction measurements using gamma ray markers, NAM, Pepijn Kole, June 2015
2. Review of wireline depth precision and accuracy for the application of compaction monitoring, Pepijn Kole, NAM, Aug 2019.
3. The First Year of Distributed Strain Sensing (DSS) - Monitoring in the Groningen Gas Field, Shell and NAM BV, M. Cannon and P. Kole, June 2018.
4. Analysis of and learnings from the first four years of in-situ strain data in Zeerijp-3A, Shell and NAM, Pepijn Kole, Matt Cannon, Jelena Tomic, Stijn Bierman, February 2020.
5. Special Report on the Garrelsweer Earthquake 16th November 2021 with Magnitude ML = 3.2, Jan van Elk en Jeroen Uilenreef, November 2021.
6. Supplement to Special Report on the Zeerijp Earthquake Swarm starting 4th October 2021, Jan van Elk en Jeroen Uilenreef, November 2021.

Title	**Zeerijp-3A in-situ Strain Analysis**	**Date**	February 2021
		Initiator	NAM
Autor(s)	Pepijn Kole	**Editors**	Rob van Eijs and Onno van der Wal
Organisation	NAM	**Organisation**	NAM
Place in the Study and Data Acquisition Plan	Study Theme: Reservoir Compaction Comment: Reservoir compaction is an important factor for subsidence and has therefore been studied since production from the Groningen field commenced. Most compaction monitoring relies on (indirect) measurements of subsidence through optical levelling surveys, GNSS and InSAR. Compaction is then derived either through direct inversion or through compaction models calibrated to these subsidence measurements and/or compaction measurements on core samples. In Groningen also in-situ measurements of compaction in the reservoir have been taken by logging the relative movement of gamma-ray markers placed in monitoring wells since 1982. In 2015 a fibre-optic cable was installed in well ZRP-3. This allows real-time continuous in-situ monitoring of compaction. As reservoir compaction is also an important input into the seismological model, the studies into seismicity in the Groningen gas field have led to an intensified interest in compaction. In 2015, the existing methods as well as a newly developed method to analyse in-situ measurements of compaction in the monitoring wells were reviewed. This was followed by a more detailed review of the in-situ compaction data using gamma ray marker surveys carried out since 2015. The review focussed on the uncertainties in the compaction measurements and whether these are sufficiently accurate to monitor reservoir compaction at the desired depth and time scales. Compaction can also be measured with the new technology of fibre-optic cables. A glass-fibre cable was installed over the reservoir section of the Zeerijp-3 monitoring well. A year after taking this in-situ compaction measurement system into operation a report describing the first year of experience with this new technology was published. The experience in measuring compaction using this system over the first four years of operation was reported in February 2020. The acquired dataset is discussed with attention to a number of significant events taking place in these four year, a coiled tubing clean out (CTCO) of the monitoring well, an earthquake of magnitude 3.4 occurring less		

	than 1.5 km from the well, an upgrade of DSS interrogator module, and multiple periods of active geophone operation. The current report extends the analysis until 31st December 2021. Special attention is given to potential compaction changes during a swarm of earthquakes at approximately 1 km from the well between 4th and 6th October 2021. An almost continuous compaction dataset has been acquired from 2015 when the Zeerijp-3A well was taken in operation until 31st December 2021. This data set has been made available by NAM through EPOS (European Plate Observatory System). The continuous acquisition of in-situ compaction measurements in the Zeerijp-3A well is carried out as part of the monitoring of the Groningen field.
Associated research	(1) Development of compaction models based on core measurements. (2) Inversion of subsidence to derive compaction estimates. (3) Seismological modelling.
Used data	In-situ measurements of compaction by logging relative movement of gamma-ray markers installed in observations wells.
Associated organisations	Baker Hughes.
Assurance	Internal.

ZEERIJP-3A IN-SITU STRAIN ANALYSIS

By Pepijn Kole
Reviewed by Rob van Eijs and Onno van der Wal
EP202204200435

SUMMARY

The strain signals are updated up to 31 December 2021, to complement earlier reports describing the data up to 2019 [1, 2]. The current report will be kept ‘evergreen’, issuing frequent updates to include newly acquired data.

The strain rates and patterns across the different formations to end-2021 are in line with those observed previously (about 25microstrain/year in ROSLU, about 15microstrain/year in ROSLL).

A series of earthquakes have been recorded near the Zeerijp location in 2021. These events do not coincide with any changes in strain throughout the DSS interval.

The DTS and DSS data show some periods of instability throughout 2021. At one instance in September 2021, the temperature in the whole wellbore appears to drop by about 0.25 ^{o}C as recorded by DTS, accompanied by a compressive strain step from DSS data analysis. In November, a more significant temperature drop is recorded by DTS (1 ^{o}C), and the downhole temperatures remain unstable afterwards. The DSS also shows instability during these sudden temperature changes. The November instance is believed to be related to a failing temperature control of the data cabin on the well site, causing anomalous readings on both the DTS and DSS.

TABLE OF CONTENTS

INTRODUCTION

A Baker Hughes fibre optics system (SureView) including distributed strain sensing (DSS) was installed in the Zeerijp-3A well in 2015 to record in-situ strain continuously. Earlier reports are available that detail the strain analysis over the first year [1] and first four years [2] of the system being operational.

While the recorded strain contained strong components from the well settling in the early phase after well completion that masked the formation strain [1], the data across the reservoir has since been confidently linked to actual reservoir deformation [2].

The current report covers the data over 2021, which was obtained after the last reported analysis. The report first contains a discussion of the stability of both the DTS and DSS, followed by the strain development across the main formations in Zeerijp-3A (Zechstein, Ten Boer, Slochteren and Carboniferous), and closes with an analysis of the strain during a sequence of earthquakes that were recorded in 2021 nearby the Zeerijp location.

DATA STABILITY

Signal stability is important to maintain confidence in the relation between measured and true formation strain. Thermal stability and reliable downhole temperature measurements are also important as the DSS data needs to be corrected for temperature changes in case these are significant [1]. Here, the DTS data stability over 2021 is discussed first, followed by an overview of the DSS stability.

DTS – temperature instability

Temperature has been assumed stable over the DSS section in earlier analysis [1, 2]. During 2021, however it has been noticed that the (apparent) temperature as recorded by DTS has not been as stable as required for reliable DSS measurements.

During 2021, there are two instances during which a significant temperature drop has been recorded by DTS for the full wellbore. The first track in Figure 1 shows the absolute temperature over time (end-2020 to end-2021), while the second track shows the temperature change, focusing on a timeframe July – December 2021. Clearly visible are two sudden drops in temperature, the first around 11 September, marked as (1) in Figure 1, and the second around 8 November 2021, marked as (2) in Figure 1.

The two instances of a sudden drop in the apparent temperature are clearly visible in Figure 2, showing the average temperature for a number of depth intervals over time. After the temperature drop that started around 8 November 2021, the temperature has remained less stable than usual.

The DTS unit has a reference coil inside the interrogator itself, used as a reference temperature and to monitor the ambient temperature of the unit. The data from the reference coil is plotted in Figure 3, and clearly shows that the ambient temperature has risen significantly after 8 November, exceeding 40°C at times and fluctuating in the range 35-40 °C while previously stable around 25°C.

The changes in the apparent downhole temperature appear to correlate very well with the changes in the reference coil, as seen in Figure 4. It is therefore likely that the high and instable ambient temperatures of the DTS unit are causing these downhole fluctuations and that these downhole fluctuations in temperature are not actual changes in the downhole environment.

The maintenance logs show that the air-conditioning unit in the data cabin has been serviced on 8 November. It is likely that the unit has not been returned to control the temperature in the room as it did prior to this, and that the high and unstable ambient temperatures are causing the instability in the downhole measurements. The issue has been reported, and the temperature control was restored on 26 January 2022. The importance of having stable temperature control will be stressed for future maintenance on site.

No known activity has taken place in the data cabin around 11 September 2021, and no data is available from the reference coil, so the cause of the data instability in September is yet unknown.

What is also visible is a continued cooling around 950-1000mAH, just below the shoe of the 13-3/8” casing (depth of the feature indicated by (A) in Figure 1). There are two different cooling patterns visible over time around this area since the start of the measurements. The pattern in depth and time makes for an interesting dataset for further analysis into the thermal behaviour of the well and annuli, but this is not included in any of the analysis here as the absolute change in temperature is minimal (<2 ^{o}C), and the shallow depth of the feature means any changes in temperature here will not affect the DSS data.

Two other features that stand out are caused by the downhole setup (locations of H-splices) and recorded temperatures at these depths have been known to exhibit anomalous behaviour [1, 2]. The depths of these features are indicated by (B) and (C) in Figure 1.

The temperature drop in November appears to be more significant at and below the H-splice at around 3633mAH, Feature (C) in Figure 1. It is believed that these are due to the setup and do not reflect actual changes in downhole temperature.

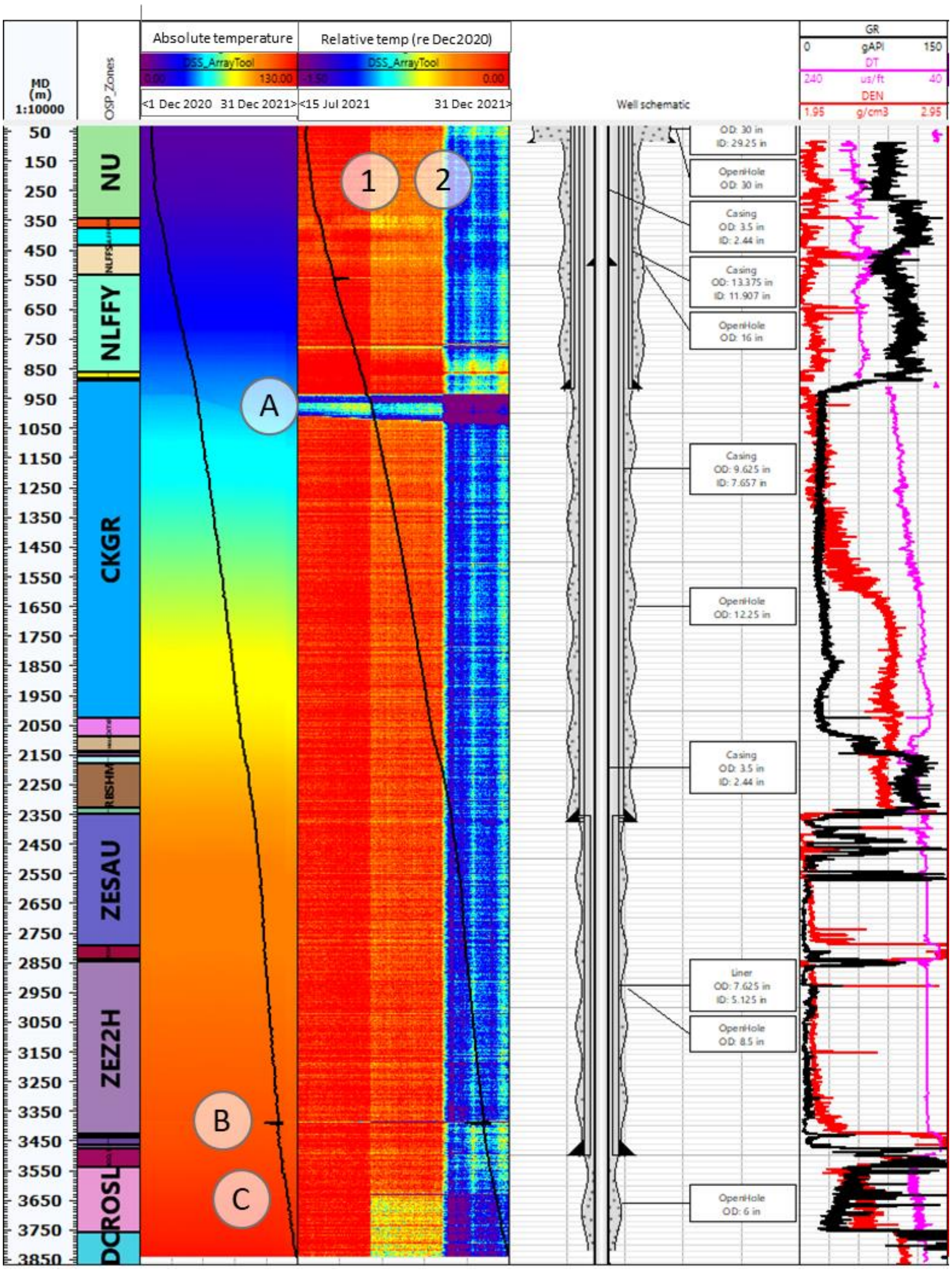

Figure 1: Temperature data from December 2020 till January 2022. The first colour map shows the absolute temperature in ^{o}C, while the second shows the temperature change since December 2020. Clearly visible are two sudden changes in temperature across the full well, the first occurring around 11 September 2021 and the second around 8 November 2021. The temperature drop in September is about 0.25 ^{o}C. A slightly higher temperature drop is seen below the depth of the H-splice, at 3633m.

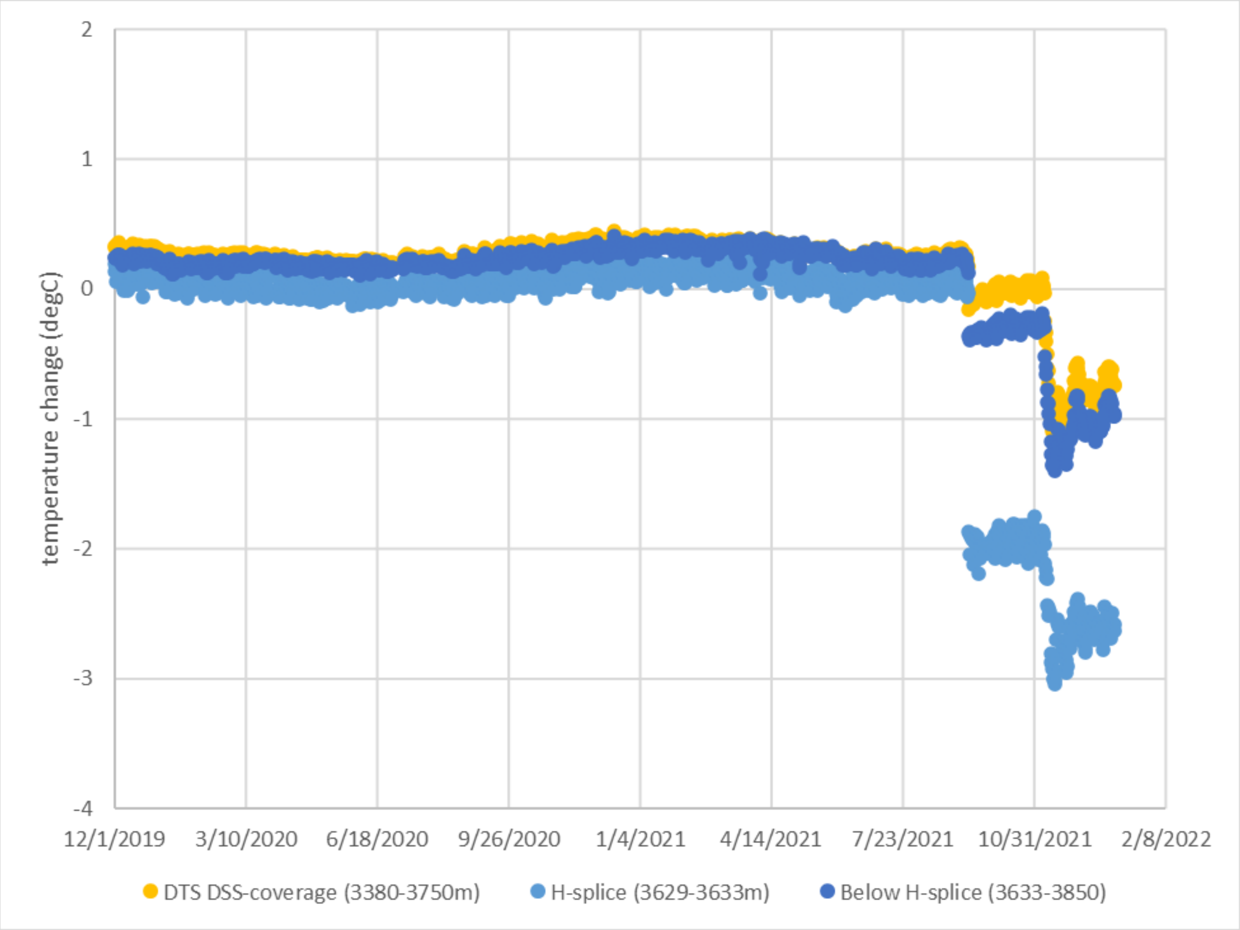

Figure 2: Average temperature change (relative to 12 October 2015, start of measurements) over three depth intervals. All three show the drop in temperature in September 2021, followed by a futher drop in November 2021, after which the temperature remains unstable.

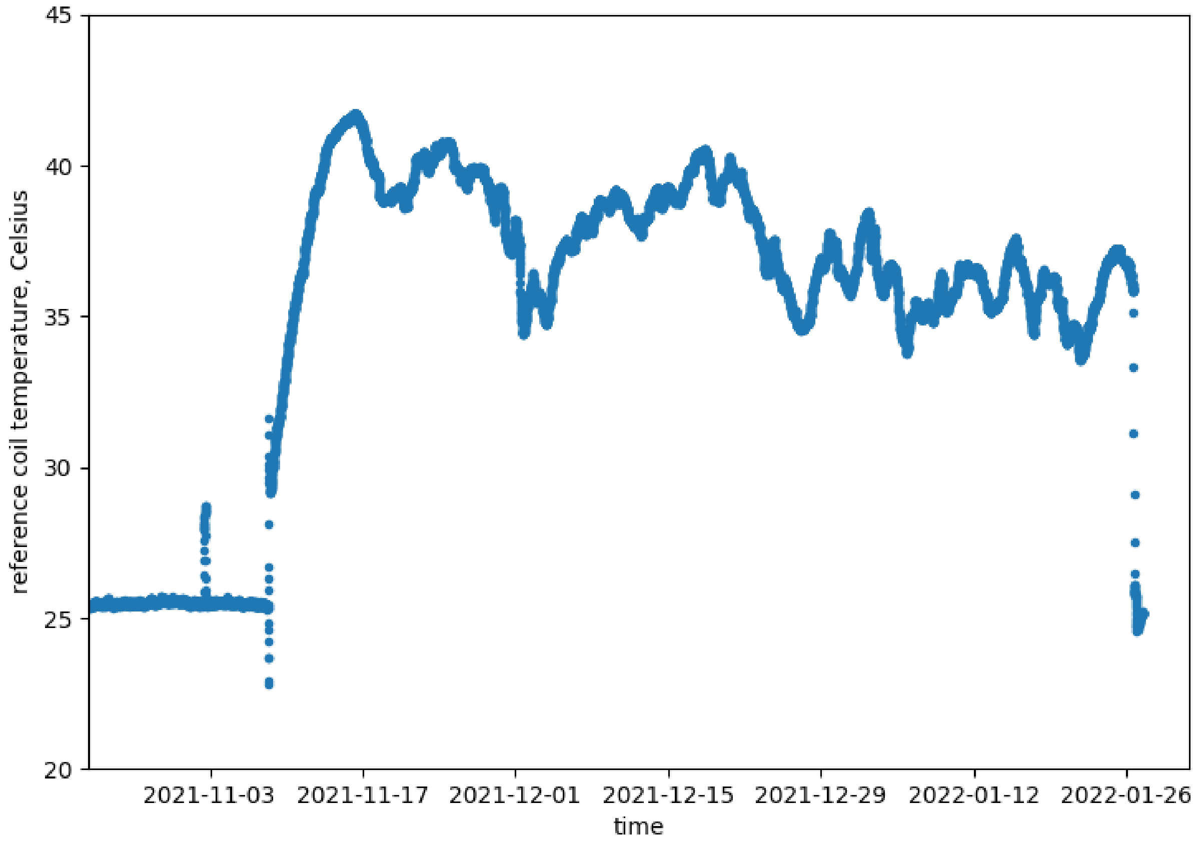

Figure 3: Temperature recorded by the reference coil, which reflects the ambient temperature of the DTS interrogator inside the data cabin at the well site. A brief temperature increase is seen to occur on 2 November 2021, but a stable 25 °C was maintained shortly after. On 8 November 2021, however, the temperature increases to over 40 °C and remains unstable, until temperature control was restored on 26 January 2022.

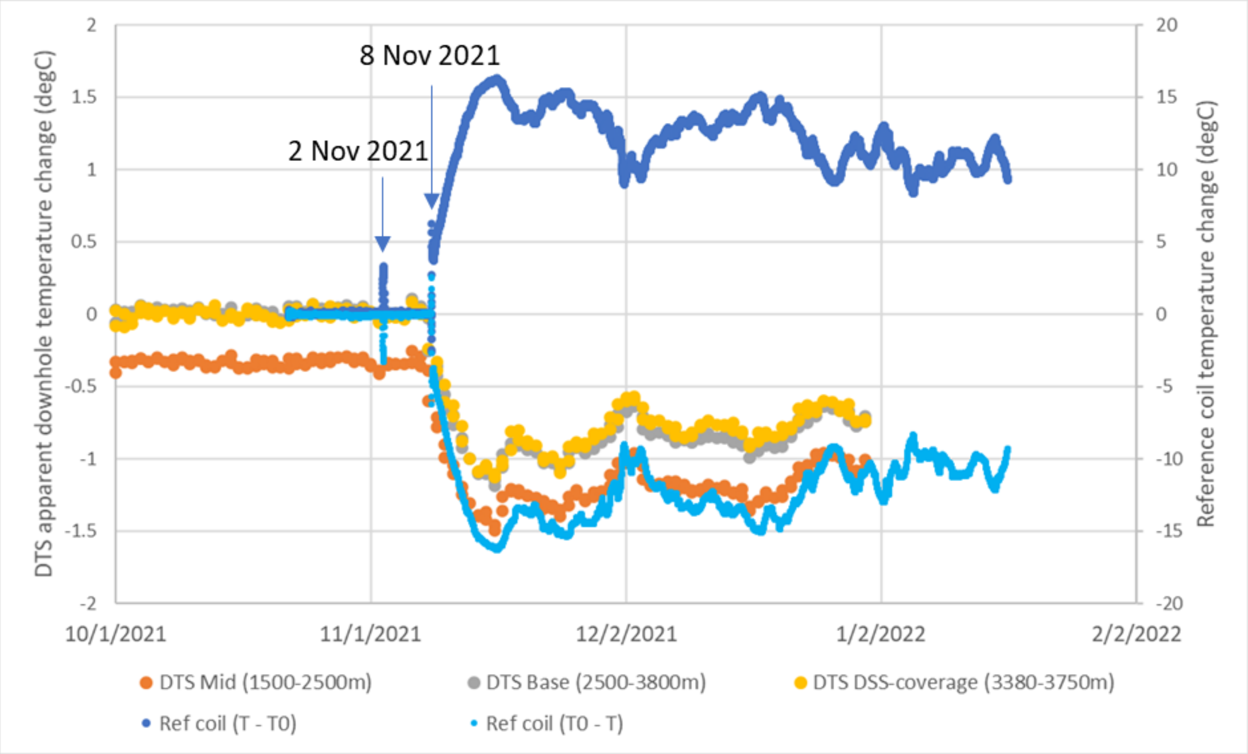

Figure 4: Apparent temperature change as recorded by DTS (left y-axis) and the change in temperature of the reference coil (right y-axis). The DTS temperature change and subsequent instability from 8 November onwards coincides with the temperature increase in the data cabin, and strongly correlates with the fluctuating ambient temperature of the interrogator.

DSS – strain stability

The strain as interpreted from the DSS data is plotted for all four Channels in Figure 5, over four depth intervals. A sudden change is visible in all channels around 10-14 September 2021 (a compressive signal), while another sudden change is observed in Channel 1 and Channel 3 around 7-11 November 2021.

As discussed in relation to the DTS stability, the DTS signal has shown instability around these two separate time intervals as well. The temperature drop in September was, roughly, 0.2-0.4 °C, while the drop in November was about 1 °C.

The strain signal in September is 0.3 to 2.0 microstrain (compressional) across the four Channel (Channel 3 appears to show the most, around 2.0 microstrain). Using the temperature correction coefficient for the DSS cable of 5-8microstrain/ °C (based on CTO event data in Zeerijp, [2]. Data from injector wells shows a similar 6.5microstrain/ °C, [1]), the amount of strain could be explained by an actual change in temperature across the well, which would result in an (apparent) compressive strain of 1-3microstrain.

A sudden change is not likely though – as previous coiled tubing clean-out, one of the most invasive well interventions in Zeerijp-3A since the DSS has been installed, did not result in such a strong and prevailing impact on the DSS and DTS. Unfortunately, no ambient temperature data is available over September to investigate if an instability in the data cabin can be the cause.

The sudden strain signal in November is only observed in two channels, making it less likely these are actual strains in the well. The direction of the strain is extensional, which, unlike the September event cannot be explained by the associated temperature drop observed in November. Given the high temperatures recorded in the data cabin coincides with the change in apparent strain (from 8 November onwards, temporarily >40 °C and remaining well above 30 °C), it is likely that the high ambient temperatures have caused an instability in the DSS unit and a subsequent apparent strain.

The high temperatures have been reported and the importance of stable temperature control will be stressed for future activity on the well site. Once the temperature has been restored to a stable 25 °C, it is believed that the strains should return to the original trend, as no permanent (and real) deformation is expected to remain. Future reports on Zeerijp DSS will discuss the development of these strains related to the thermal instability.

Apart from the two sudden changes in the strain, the signal from the DSS has been stable, also between the two events in September and November, and is believed to be reliable.

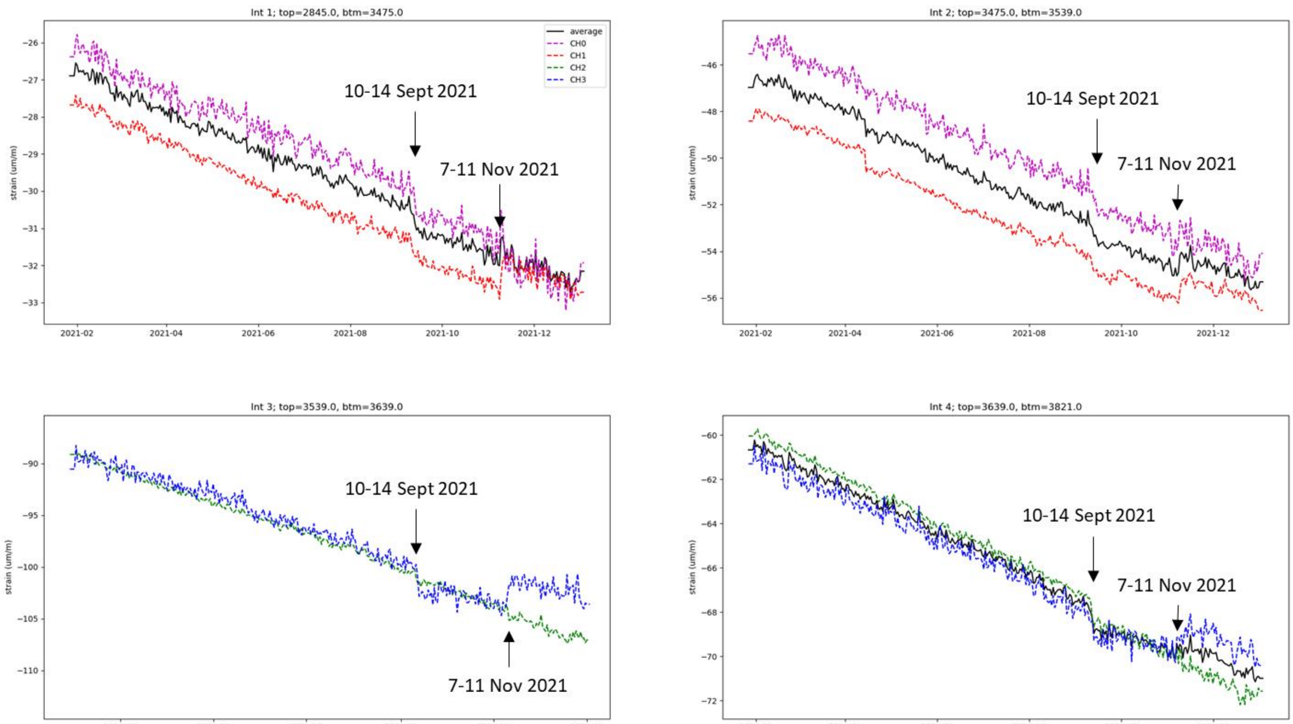

Figure 5: Strain development (relative to March 2016) throughout 2021. Each plot shows the strain within a specific depth interval (int 1: 2845-3475mAH, int 2: 3475-3539mAH, int 3: 3539-3639mAH, int 4: 3639-3821mAH).

STRAIN UPDATE – JANUARY 2022

Figure 6 shows the strain development across the main formations in Zeerijp-3A. The strain instability during September and November 2021, discussed above, is visible across all intervals. The general strain development continues at rates similar to those previously reported [2]; about 25microstrain/year in ROSLU, about 15microstrain/year in ROSLL, 10microstrain/year in ROCLT, 5microstrain/year in DC. The strain as a function of depth is plotted in Figure 7.

In previous processing, the strain data had been filtered to remove data affected by significant changes in the wellbore environment (e.g. during active geophone installations, coiled tubing clean out operations, [2]). As the impact of such events is expected to decay away over time and to not leave any permanent deformation, the current report has kept all such data to stay as close to the raw data as possible. The data below, therefore, includes strain signals caused by thermal effects from geophones and well interventions.

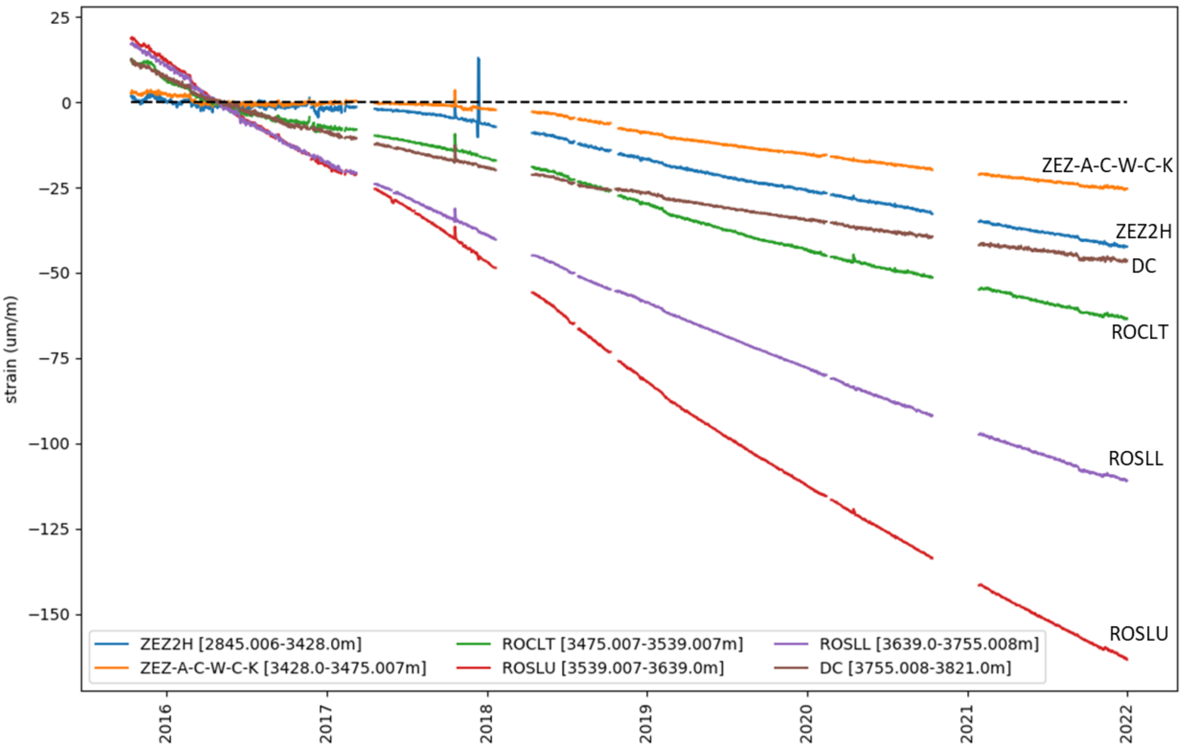

Figure 6: Strain over time for different formations in Zeerijp-3A.

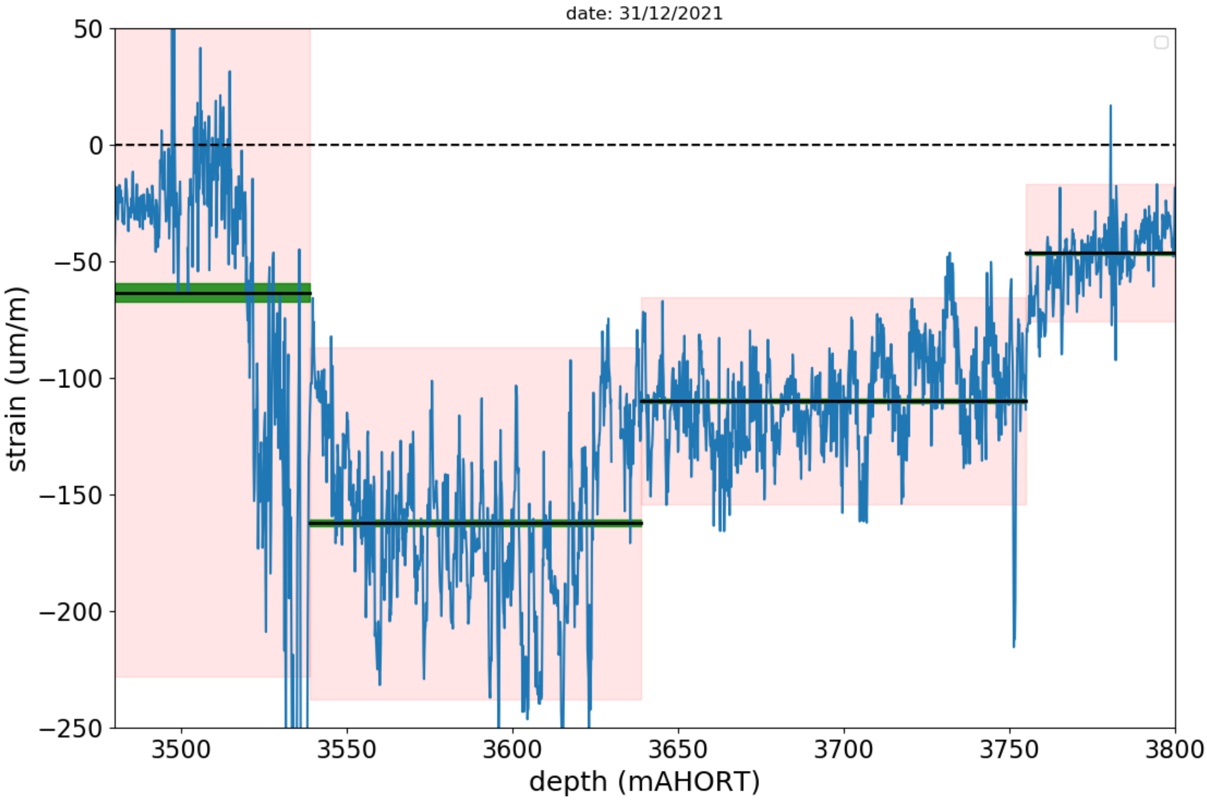

Figure 7: Accumulated strain until 31 December 2021 as a function of depth. The measured strain is plotted in blue. The black lines show the average interval strain (for ROCLT, ROCLU, ROCLL, and DC), the green bands the uncertainty in the average and the pink shaded area indicates the spread of strain within and interval (2 standard deviations).

Zechstein

A clearly non-zero, compressive strain is also visible in the Zechstein units. The strain data shows intervals of compressive strains on both Channel 0 and Channel 1, in-phase, meaning that the signal is not due to bending of the DSS cable but more of an actual compressive strain of the DSS fibre.

The accumulated strain until 31 December 2021 is shown in Figure 8, together with log data from Zeerijp-3A. The strain curve does not show a clear correlation with formation logs, but it does show some correlation with the calliper and the measured bond index of both the 3.5” and 7” casings, where the lower bond index intervals appear to accumulate more strain (note that the bond index as derived from CBL data is not representative for the actual cement coverage over anhydrite intervals, as the sound velocity there is faster than through the casing itself, and as a result the CBL amplitudes do not reflect the casing attenuation).

It has to be noted that the DSS cable is not in an annulus adjacent to the formation but is inside another casing (7”) and annulus. The DSS system has never been tested in between two casings. As a result, the effect of the setup over this section on the relation between measured strain and actual formation strain is not accurately known and it cannot be guaranteed that the measured strain is representative for the actual formation strain inside the 7” casing.

Before linking the strain signals over the Zechstein to actual formation strain, the influence of the well configuration has to be considered. A schematic overview of some important mechanical features that can potentially influence the link between formation dynamics and strain recorded by the DSS cable is given in Figure 9.

For example, one could imagine that a poorer cement can allow for compression of the cement and 7” casing (and translated to strain on the 3.5” casing) under the weight of annular fluids near the top of cement, and effects from the mobile salt of the Zechstein formation. Similarly, washouts and cashing shoes can be expected to cause movement of the casing(s) that is not necessarily related to formation strains. A more detailed study should be performed before relating the strain signals recorded over the Zechstein intervals to actual formation strain.

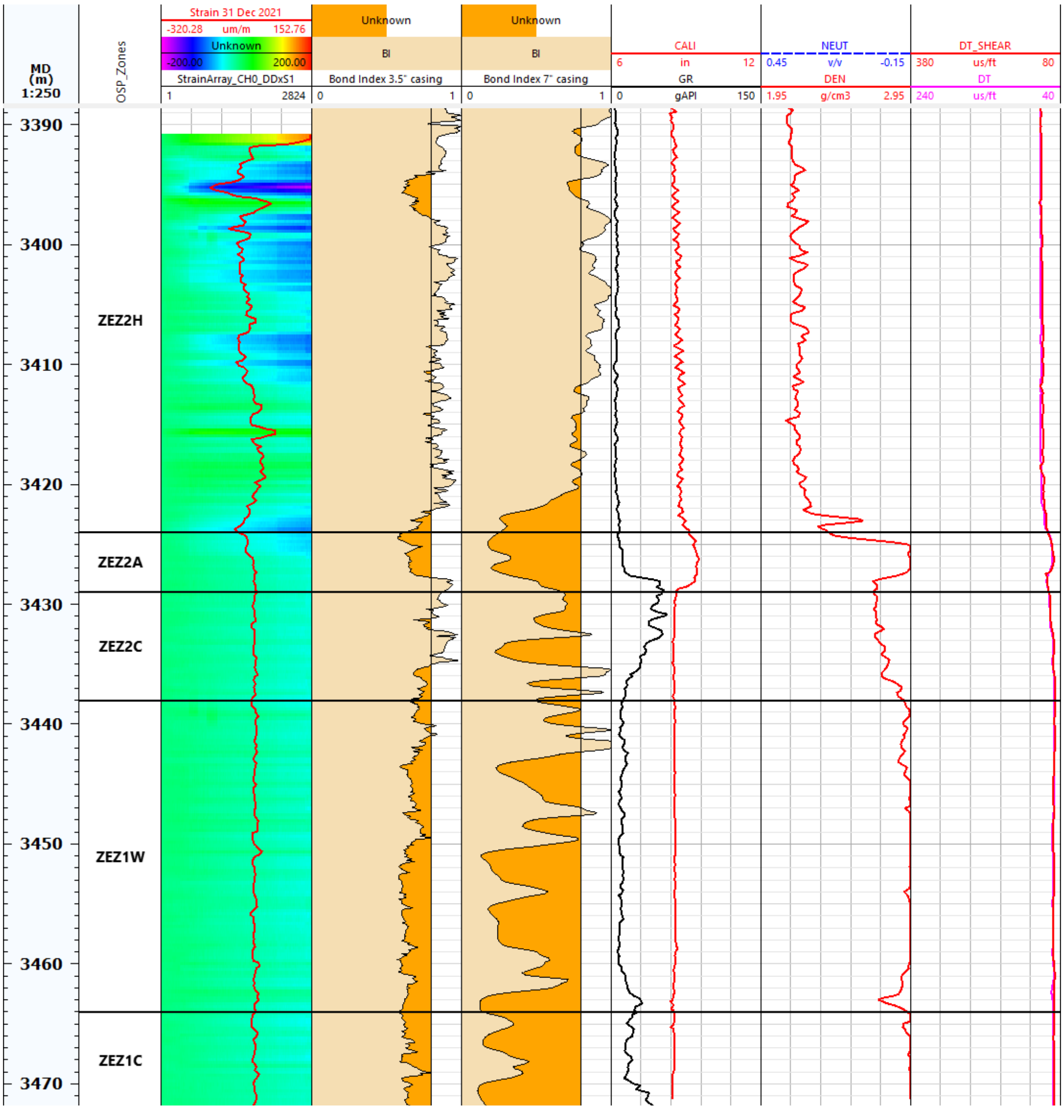

Figure 8: Interpreted strain until 31 December 2021 across the Zechstein intervals. A strain heat map and total strain curve are plotted in the first track. The other tracks show cement bond index curves and formation related log data.

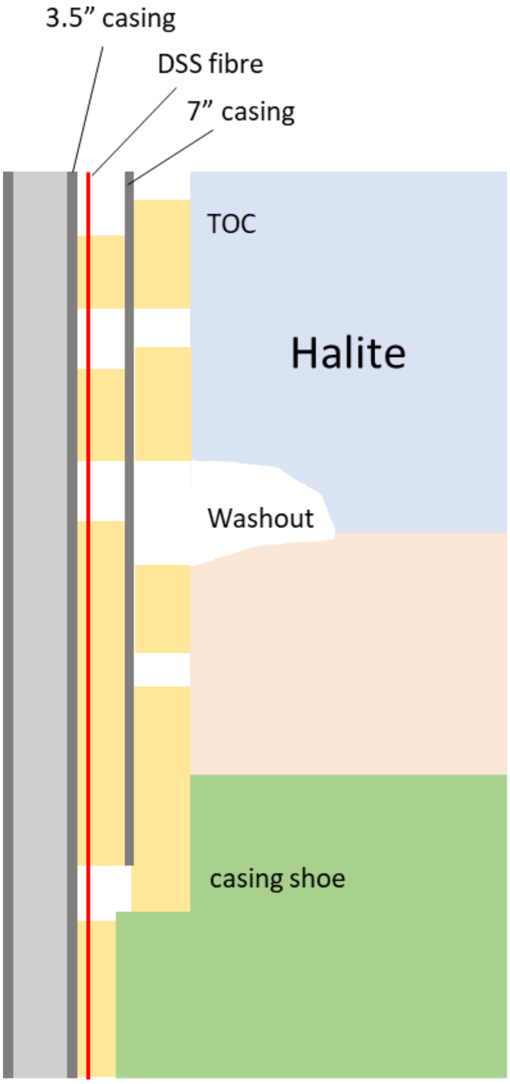

Figure 9: Schematic well layout. ***Note that the cement coverage here is for illustrative purposes and includes exaggerations, hence it does not necessarily reflect an actual cement coverage for the Zeerijp-3A well.***

Ten Boer

The strain data across the Ten Boer is shown in Figure 10. A strong compressive signal around 3500m coincides with the rat hole of the 8.5” open hole section, and correlates very well with the calliper readings. The rathole is therefore the likely cause of the significant compressive strain around 3500m.

A strong compressive strain signal around 3535m started to appear shortly after the DSS recordings had started [1] and has since continued to expand outwards. The total strain accumulated since measurements began is 300-500microstrain over this interval at the end of 2021.

It has been argued that the event was likely caused by disturbances caused by the drilling of the well, that could have allowed for pressure communication/equilibration between certain layers [1, 2].

The depth at which it started has a slightly lower bulk density reading compared to its immediate surroundings, but not anything significant to conclude that the rock is locally much softer. Some correlation with cement bond index is also noticeable.

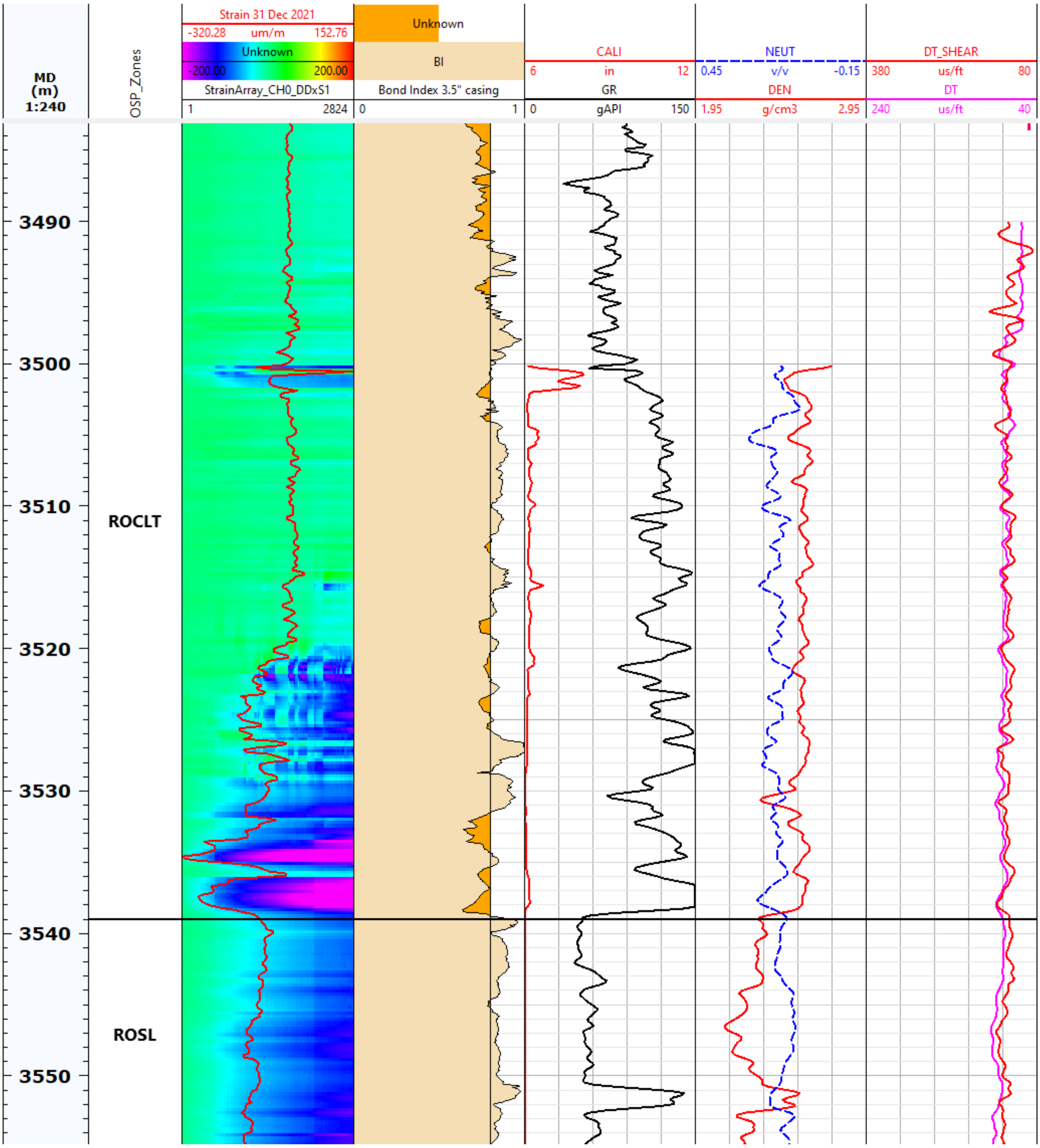

Figure 10: Interpreted strain until 31 December 2021 across the Ten Boer. A strain heat map and total strain curve are plotted in the first track. The other tracks show cement bond index curves and formation related log data.

Since 2019, some periodic signals have started to appear in the strain data of the Ten Boer above the main Ten Boer strain event, between roughly 3520-3530m. The top is close to the top of the first core, which was taken from 3521m onwards.

A subdivision based on the observed strain signals has been made to look deeper into these periodic signals. The strain and log data with these subdivisions of the ROCLT are shown in Figure 11. The strain development in each of these intervals over time is plotted in Figure 12.

The periodicity is especially pronounced in the intervals ROCLT_1 (3512.0-3521.1m), ROCLT_2 (3521.1-3521.8m), ROCLT_3 (3521.8-3524.1m), ROCLT_4 (3524.1-3525.6m) and ROCLT_5 (3525.6-3531.0m). Amplitudes of strain over these intervals are several tens of microstrains, or even close to 100 microstrains. As the intervals are relatively thin, the actual amount of movement and compaction / expansion is very small. Figure 13 shows the amount of compaction for each of the intervals. The amplitudes of the oscillations are less than 0.1mm.

There are different frequencies visible in the periodic signals. The highest amplitude features appear on a time scale of several months, the second most prominent on a scale of several weeks, and a small feature of up to 10-20microstrain is visible with a periodicity of 3-4 days.

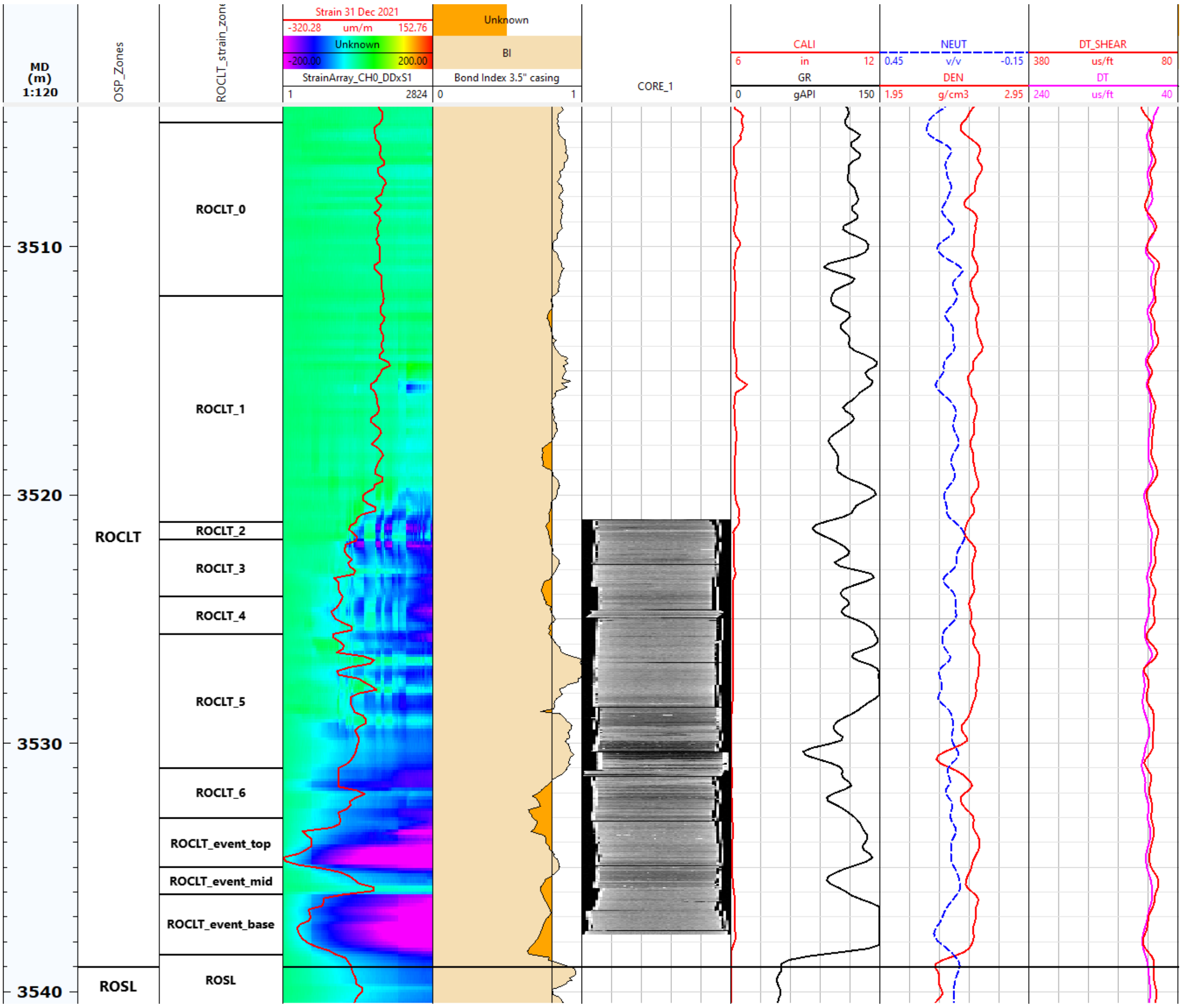

Figure 11: Strain map and curve across the Ten Boer, with a subdivision based on the strain signal annotated (ROCLT_strain_zones).

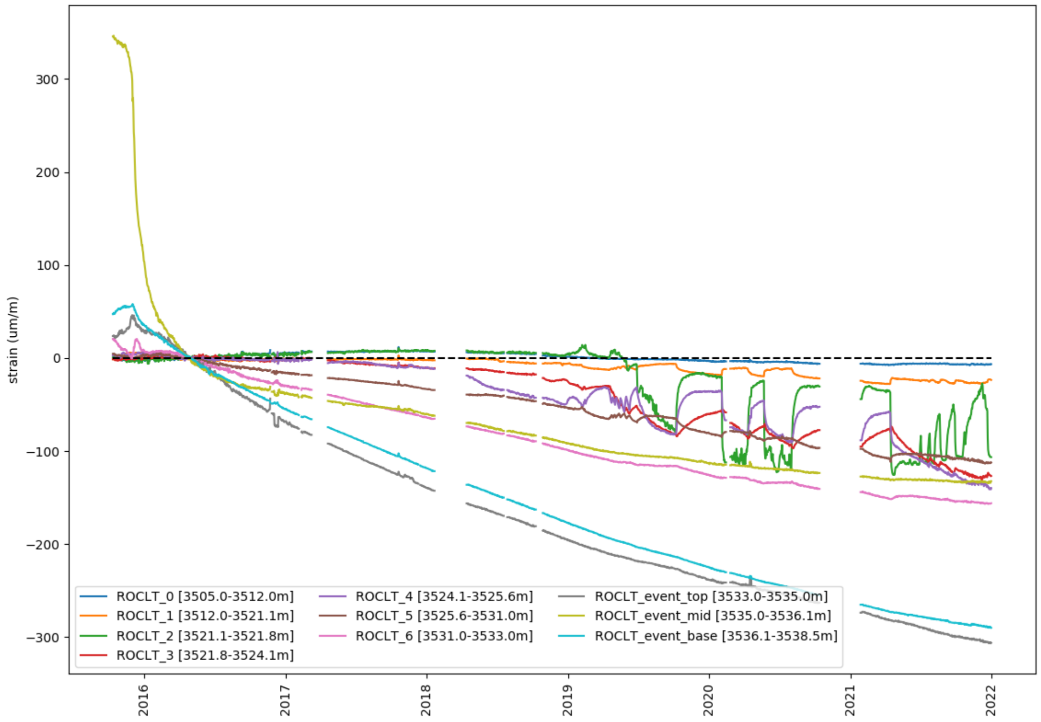

Figure 12: Strain signals over time for each of the subdivisions of the Ten Boer interval.

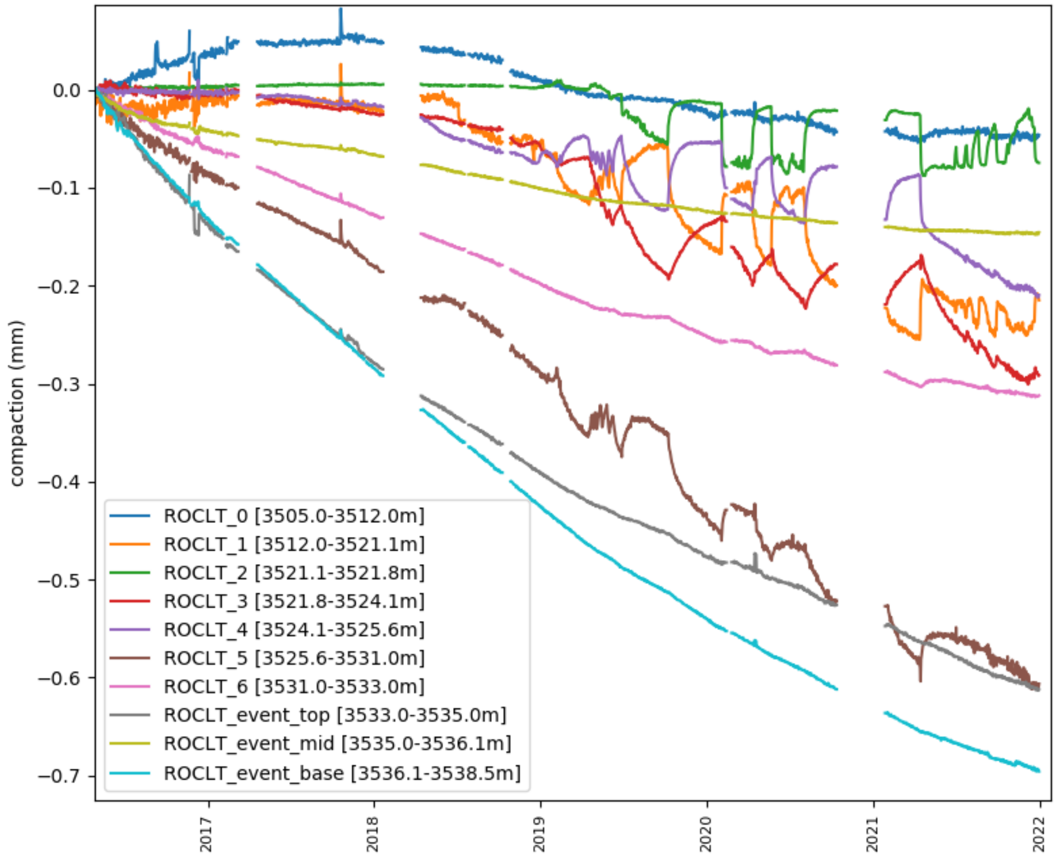

Figure 13: Compaction for a range of ROCLT intervals.

The signature of these strains over time has the characteristics of a charging and discharging phenomenon. One explanation could therefore be a local pressure communication, charging and depleting intervals in a periodic fashion.

What is striking is that the oscillatory strain signals of some of these intervals appear out of phase with one another, for example ROCLT_1 and ROCLT_5 appear to be in-phase, but out of phase with intervals ROCLT_2, ROCLT_3 and ROCLT_4.

During the out of phase behaviour between two adjacent intervals, one of the intervals contracts while the other expands, and vice versa, while the periodic strain signal cancels (almost fully) out over the combined interval. The interface between the intervals basically moves up and down. To show the amount of movement of the interface between these layers, the compounded compaction from 3505m down to the base of each of the ROCLT subdivisions is plotted in Figure 14. The compaction shown is then the movement of the base of each layer relative to 3505m.

The interface between out of phase intervals ROCLT_1 and ROCLT_2, i.e. the base of ROCLT_1 at 3521.1m, plotted in orange in Figure 14, shows a periodic movement of the interface on the order of 0.1mm, and a similar magnitude of movement for the interface between ROCLT_4 and ROCLT_5 (the base of ROCLT_4, purple line in the plot).
More detailed analysis should be done into this intriguing strain signal to better understand its cause.

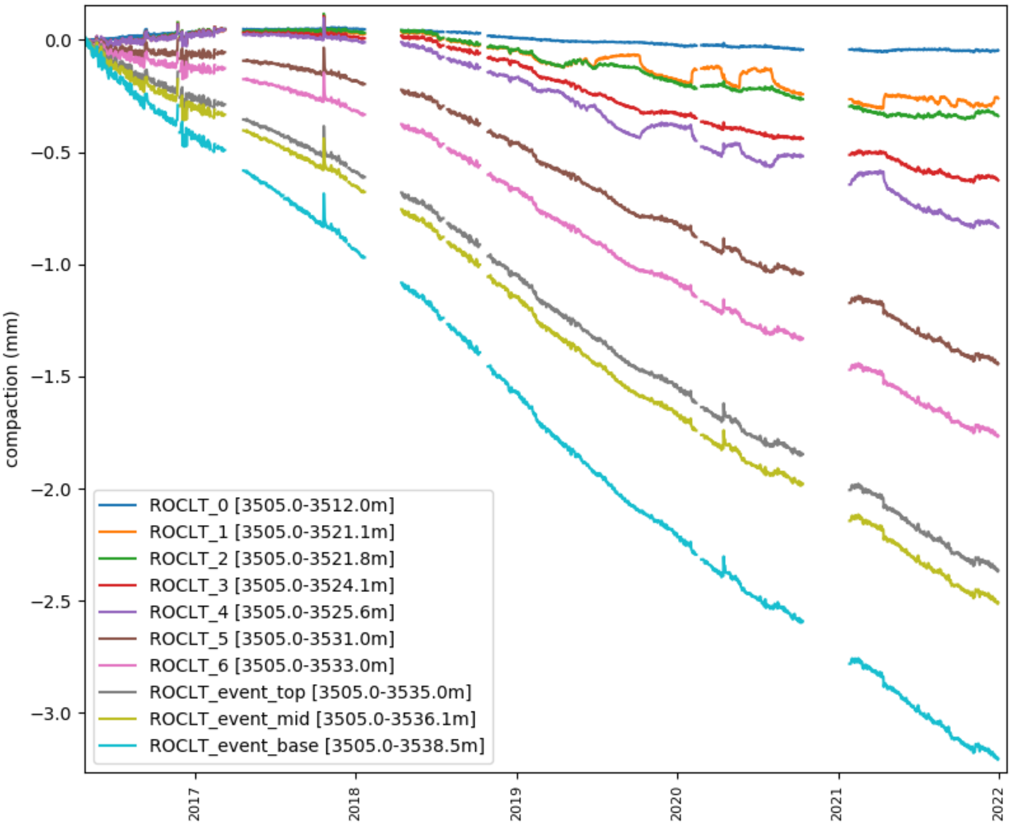

Figure 14: Compounded compaction over the different ROCLT subdivisions.

Slochteren

The strain signal over both the ROSLU (Figure 15) and ROSLL (Figure 16) continue to correlate well with formation logs, suggesting that the reservoir strain is well represented by the measured strain. In an earlier report, it was shown that the magnitude of the strain agrees well with what is expected from pore pressure depletion estimates and core compressibility data [2].

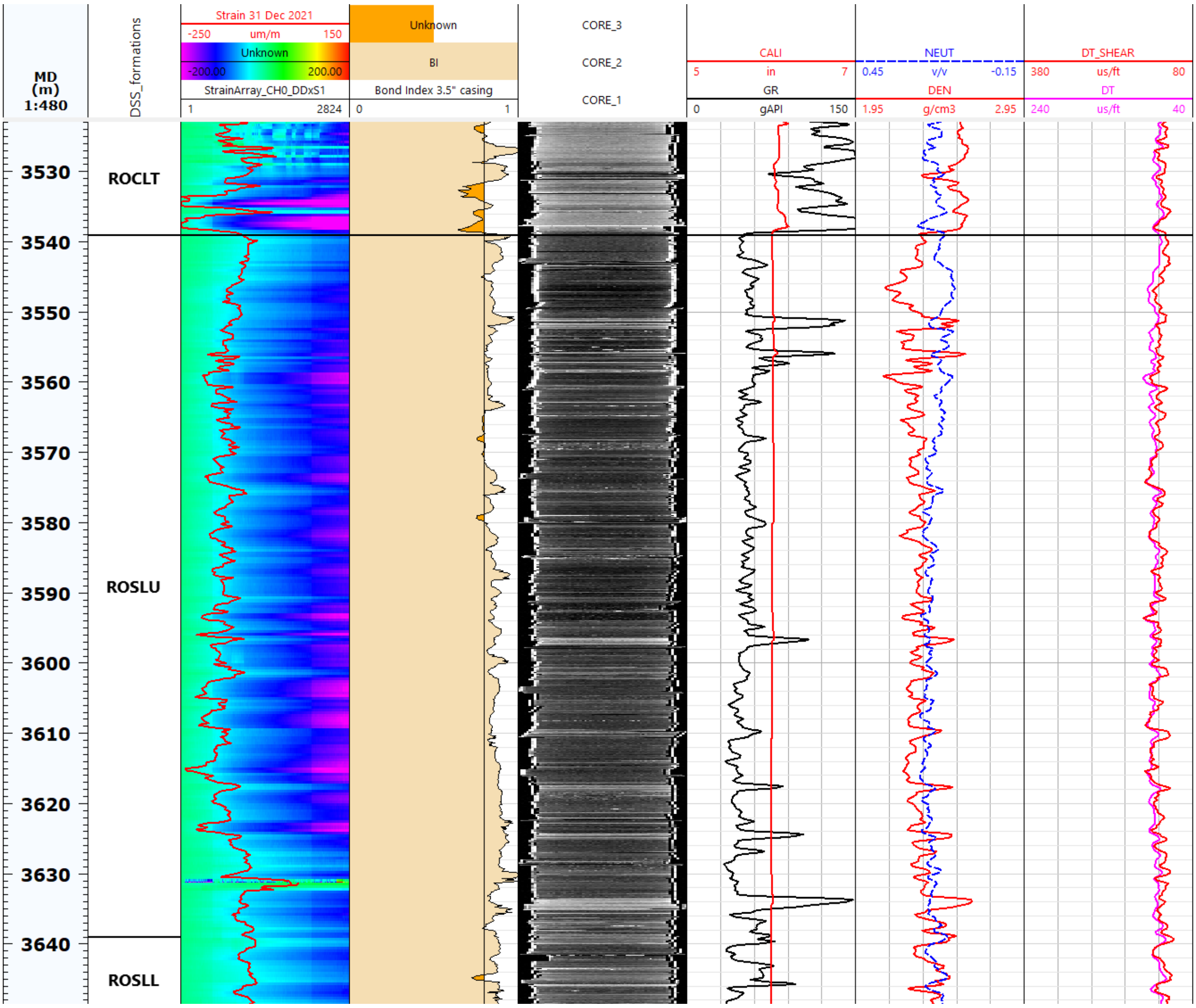

Figure 15: Measured strain, core photos and log data over ROSLU.

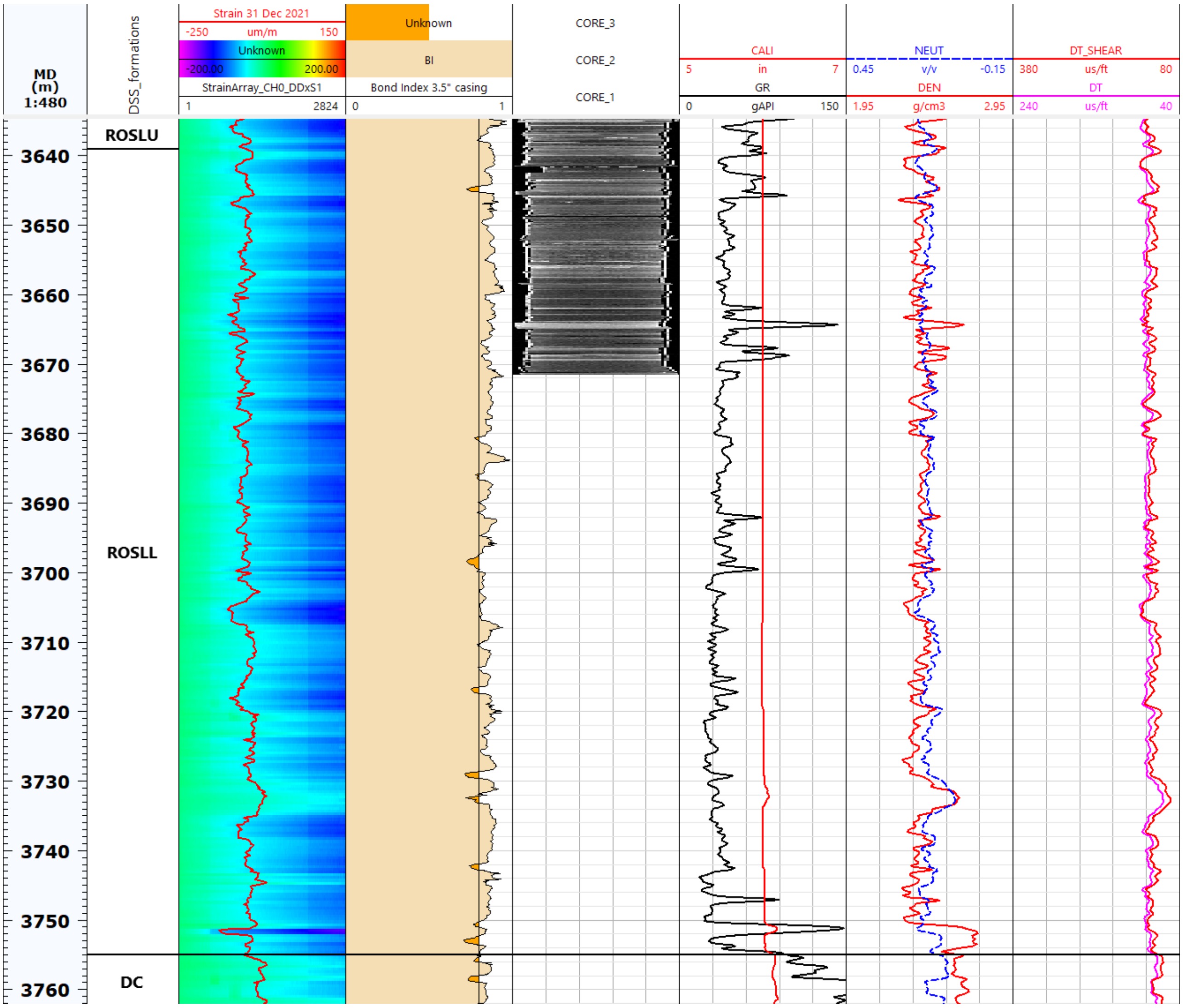

Figure 16: Measured strain, core photos and log data over ROSLL.

Carboniferous

The non-zero, compressive strain signal observed of the Carboniferous continues throughout 2021. Most of the strain is concentrated at the top of the Carboniferous, close to the overlaying Slochteren (Figure 17), and the amount of strain decays away at deeper depths, until about 3825m when the amount or recorded strain increases slightly.

Like for the Ten Boer, it is possible that some sands now deplete via the well annulus, not necessarily via the reservoir.

It is not known to what extend the signal at the deepest parts of the DSS cable is affected by it being near the base of the well, and if it is affected at all or if these are true formation strains.

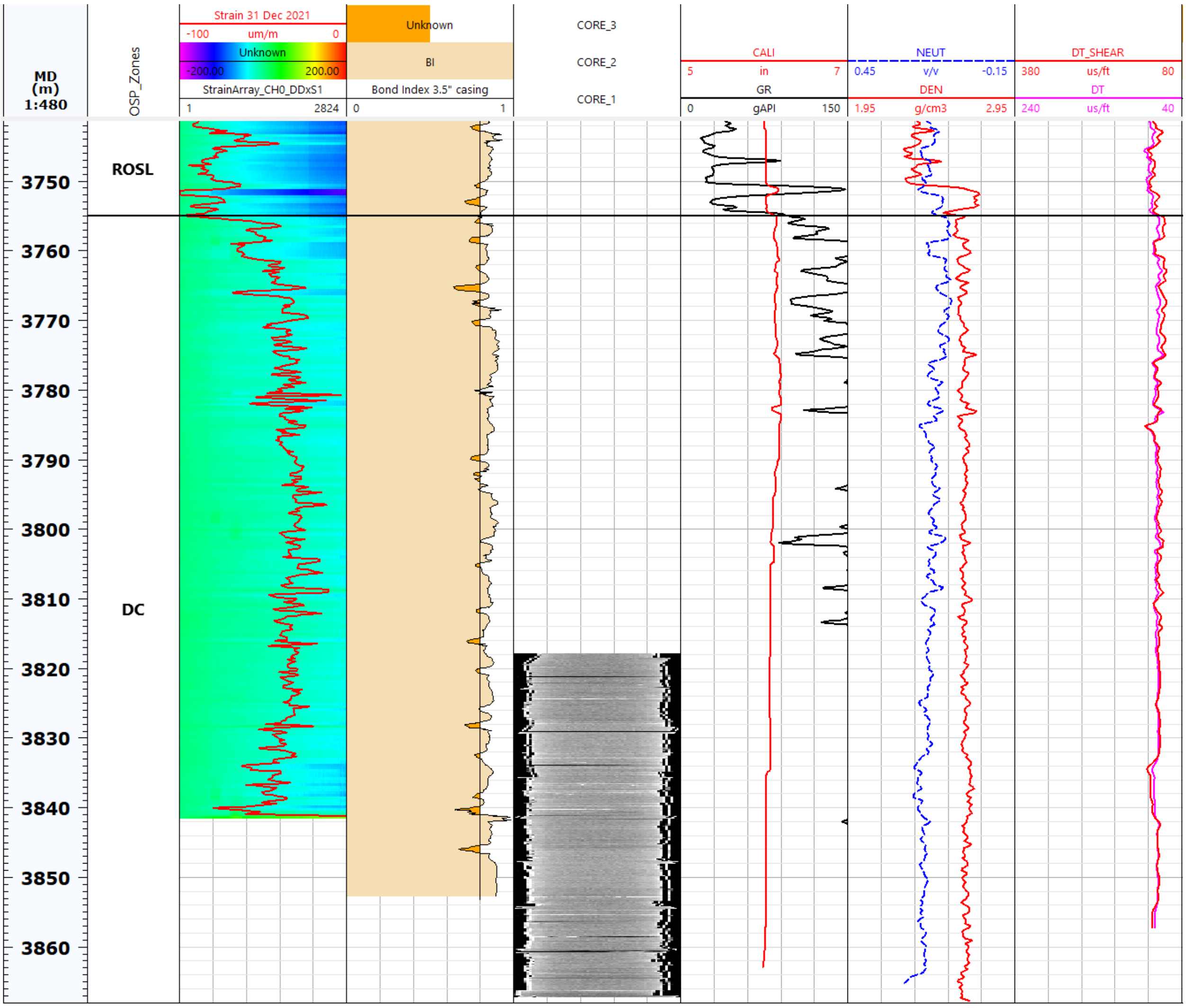

Figure 17: Measured strain, core photos and log data over the Carboniferous. Note that the scale of the strain curve has changed compared to the figures for the Slochteren.

SIGNALS DURING SEQUENCE OF 2021 ZEERIJP EARTHQUAKES

A number of earthquakes have been reported in the vicinity of Zeerijp in 2021. The DSS data around the time of the earthquakes is analysed here in more detail to verify if any signatures from the events can be seen on the measured strain in Zeerijp-3A.

The earthquakes from the KNMI catalogue [3] are visualized in an aerial view in Figure 18 and in the magnitude vs distance to the well in Figure 19. The events that took place in 2021 within a lateral distance of 1km from the DSS cable are listed in Table 1.

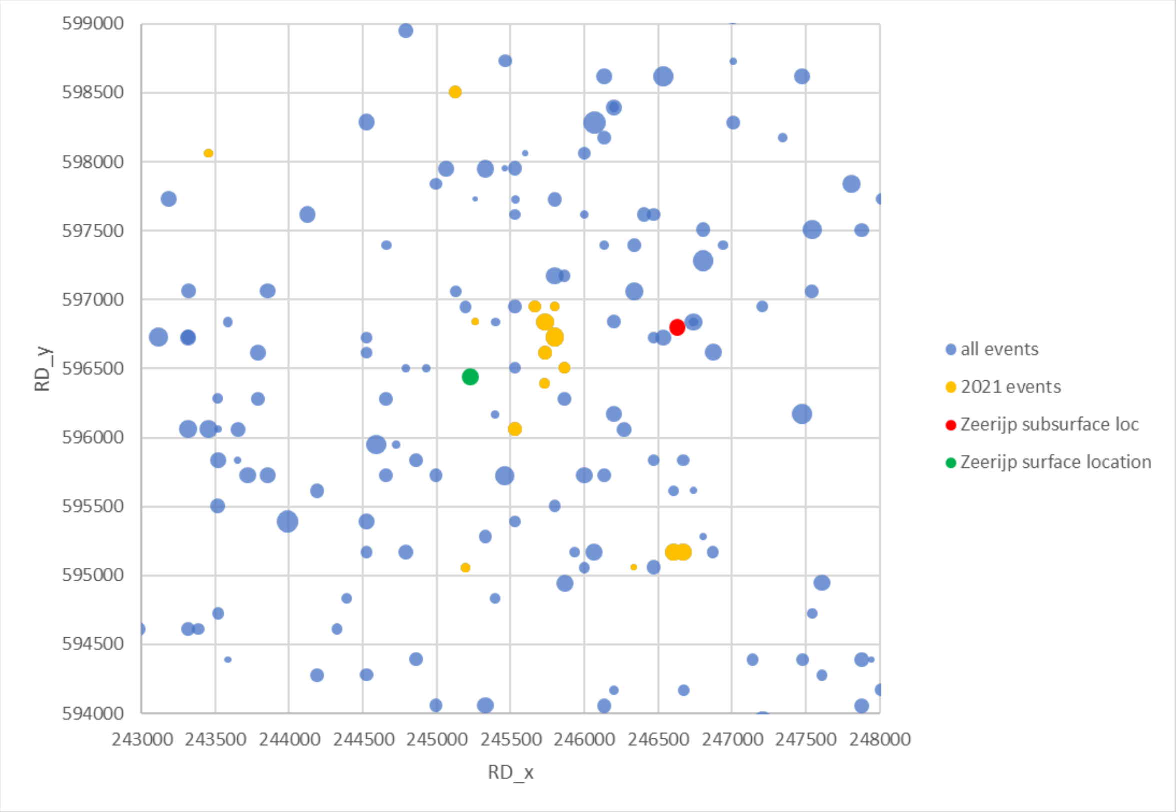

Figure 18: Aerial distribution of reported earthquakes in the KNMI catalogue. The surface and subsurface location of Zeerijp-3A are highlighted in green and red, respectively. The earthquakes that took place in 2021 are highlighted in yellow. The size of the data points reflects the magnitude of the recorded earthquakes.

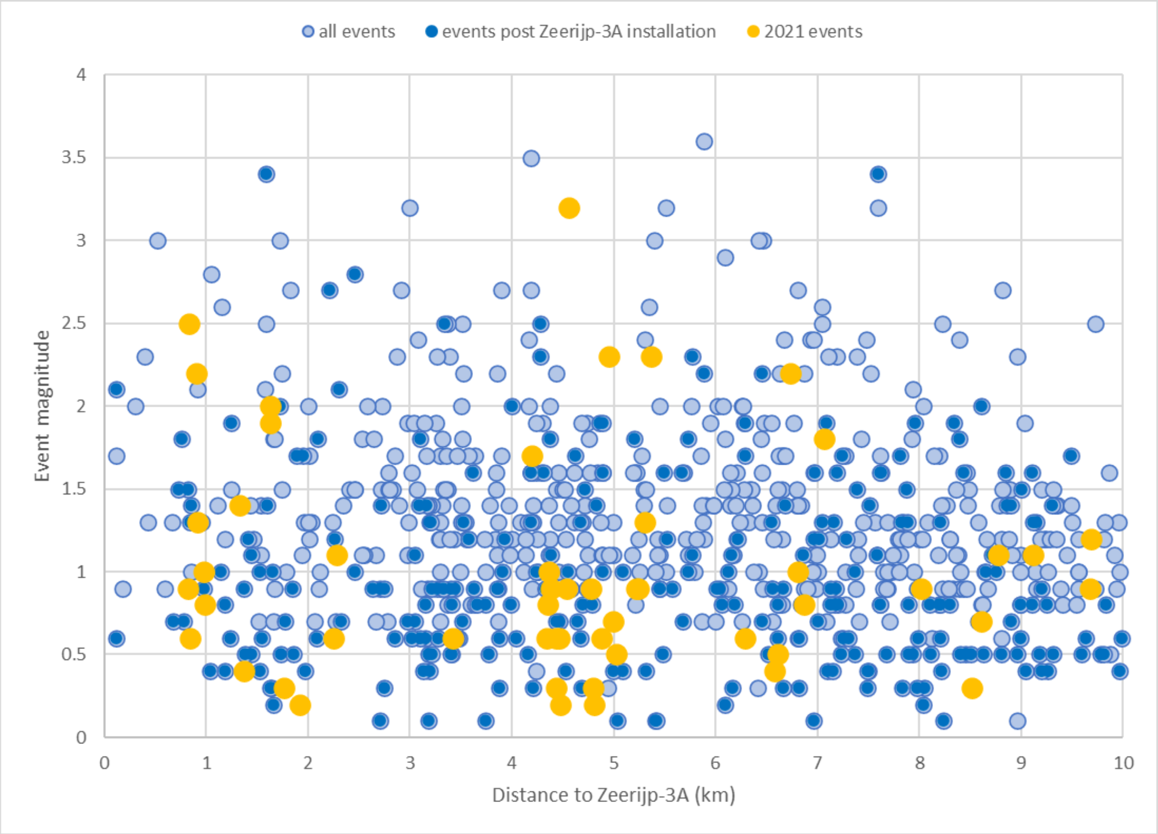

Figure 19: Magnitude and lateral distance to Zeerijp-3A (subsurface) for the earthquakes in the KNMI catalogue. Events highlighted in dark blue have taken place since the installation of DSS in Zeerijp, and events highlighted in yellow took place in 2021.

Table 1: Excerpt from the KNMI catalogue, showing events that took place in 2021 within a lateral distance of 1km from ZRP-3A.

Year	Month	Day	Event location	LAT	LON	Depth (km)	Magnitude
2021	09	18	Zeerijp	53.347	6.748	3	0.9
2021	10	04	Zeerijp	53.349	6.747	3	2.5
2021	10	04	Zeerijp	53.35	6.746	3	2.2
2021	10	06	Zeerijp	53.348	6.746	3	1.3
2021	10	07	Zeerijp	53.351	6.747	3	0.6
2021	10	15	Zeerijp	53.365	6.737	3	1.1
2021	10	22	Zeerijp	53.346	6.746	3	0.8
2021	10	27	Zeerijp	53.35	6.739	3	0.4
2021	11	13	Zeerijp	53.351	6.745	3	1.0

The strain across the main formations in Zeerijp-3A are plotted together with the timings of the near-by earthquakes in Figure 20. Unfortunately, the timing of these events coincides with the two instances of instability on the DTS and DSS data. The DSS is deemed stable in between these two instances, however, during which no strain rate changes can be observed that coincide with any of these events.

A detail of the strain in the Ten Boer is plotted in Figure 21, to compare the periodic strain features observed over certain layers. It is striking that all these events seem to occur within one period of the periodic signals in the ROCLT_2 interval (that has a periodicity of several weeks), which shows a building amplitude since May 2021, and the events occur just prior to reaching the highest amplitude. The alignment of these features is likely coincidental, as no earthquakes have occurred during similar characteristics in the strain signals. When looking at all recorded earthquakes that occurred within 1km from the Zeerijp-3A well, there is no clear correlation between the Ten Boer strain characteristics and the earthquake occurrence (Figure 22).

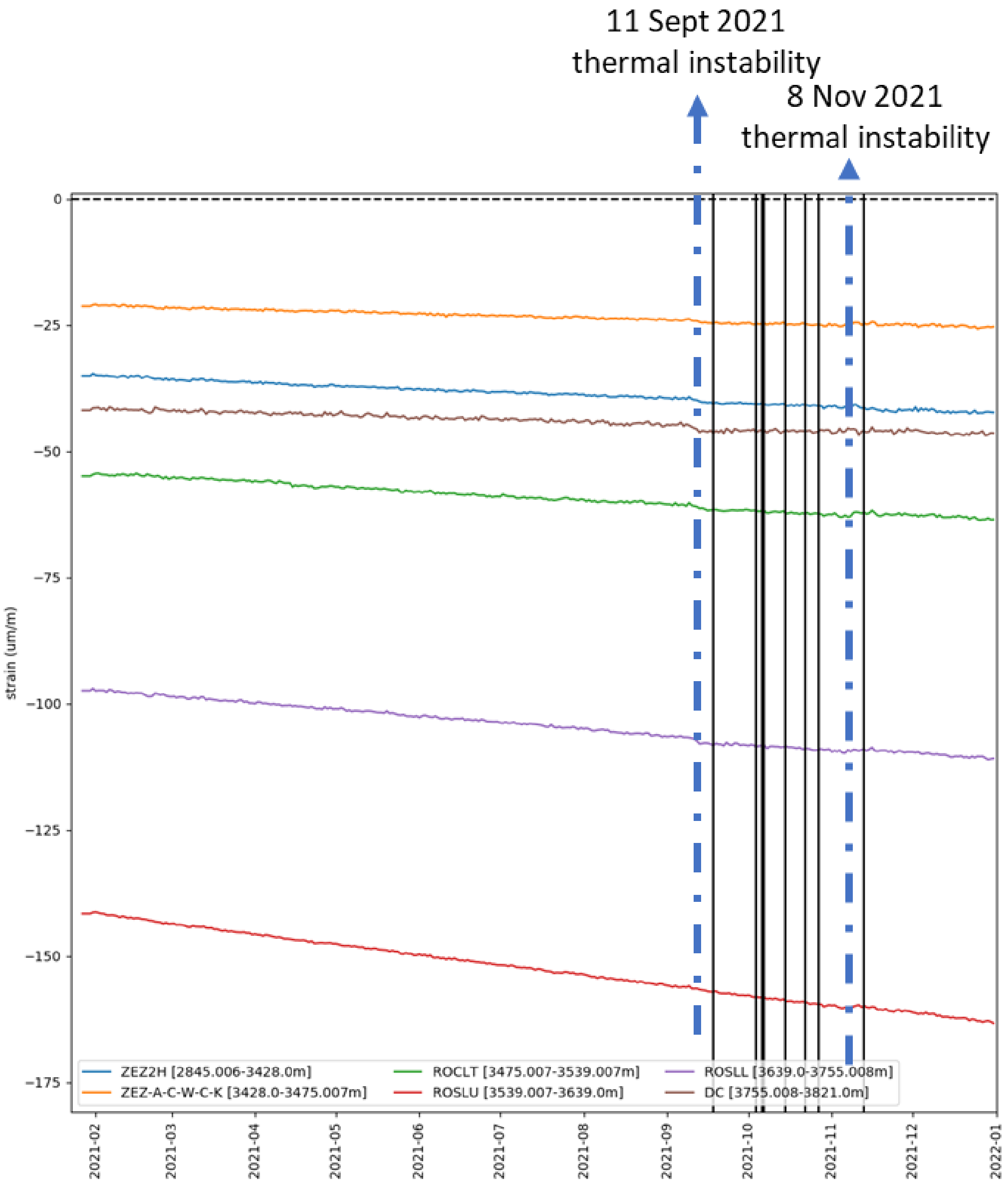
11 Sept 2021
thermal instability

8 Nov 2021
thermal instability

Figure 20: Strain signals over time for the main formations in Zeerijp-3A. Timing of the earthquakes are highlighted by the vertical black lines.

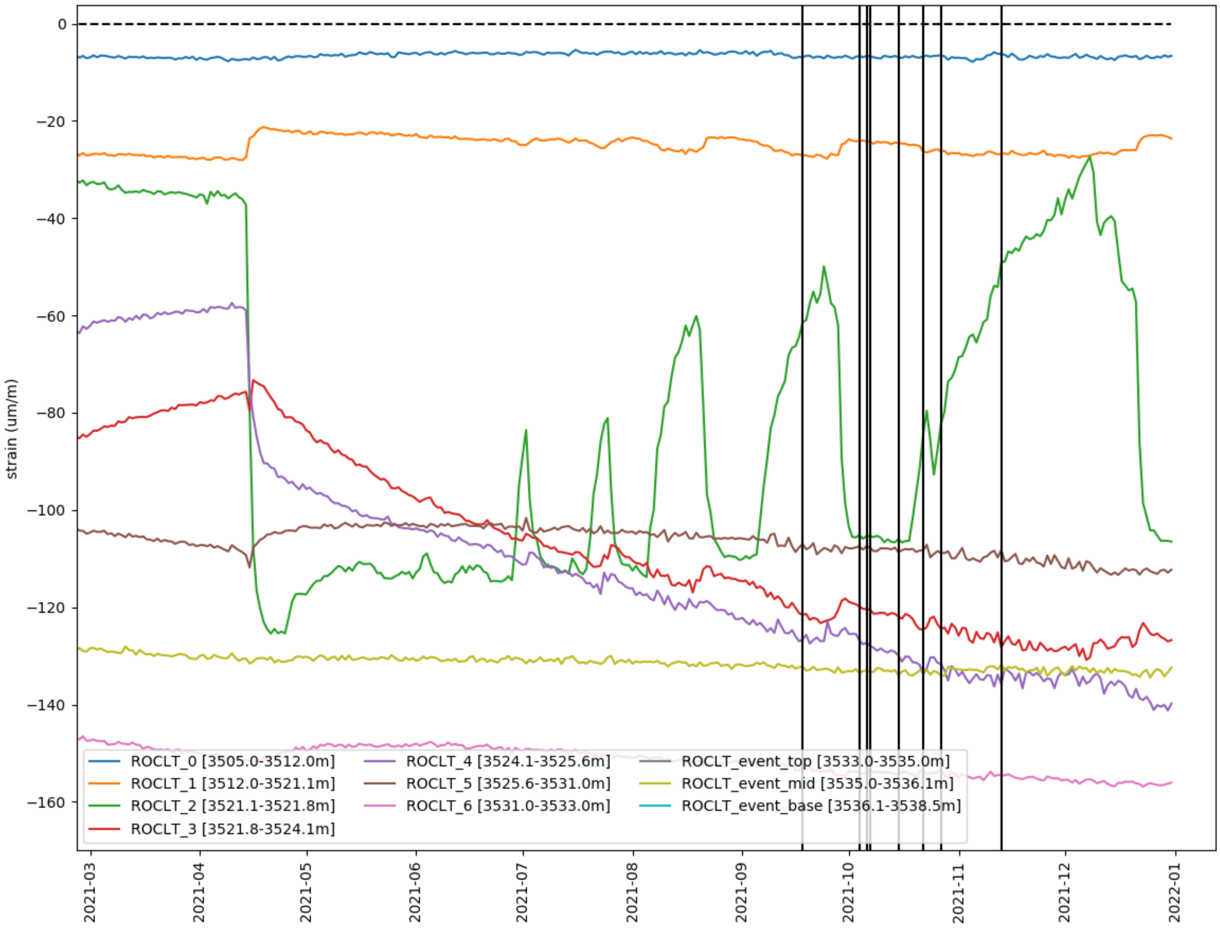

Figure 21: Strain signals over time for the subdivisions of the Ten Boer formation. Timing of the earthquakes are highlighted by the vertical black lines.

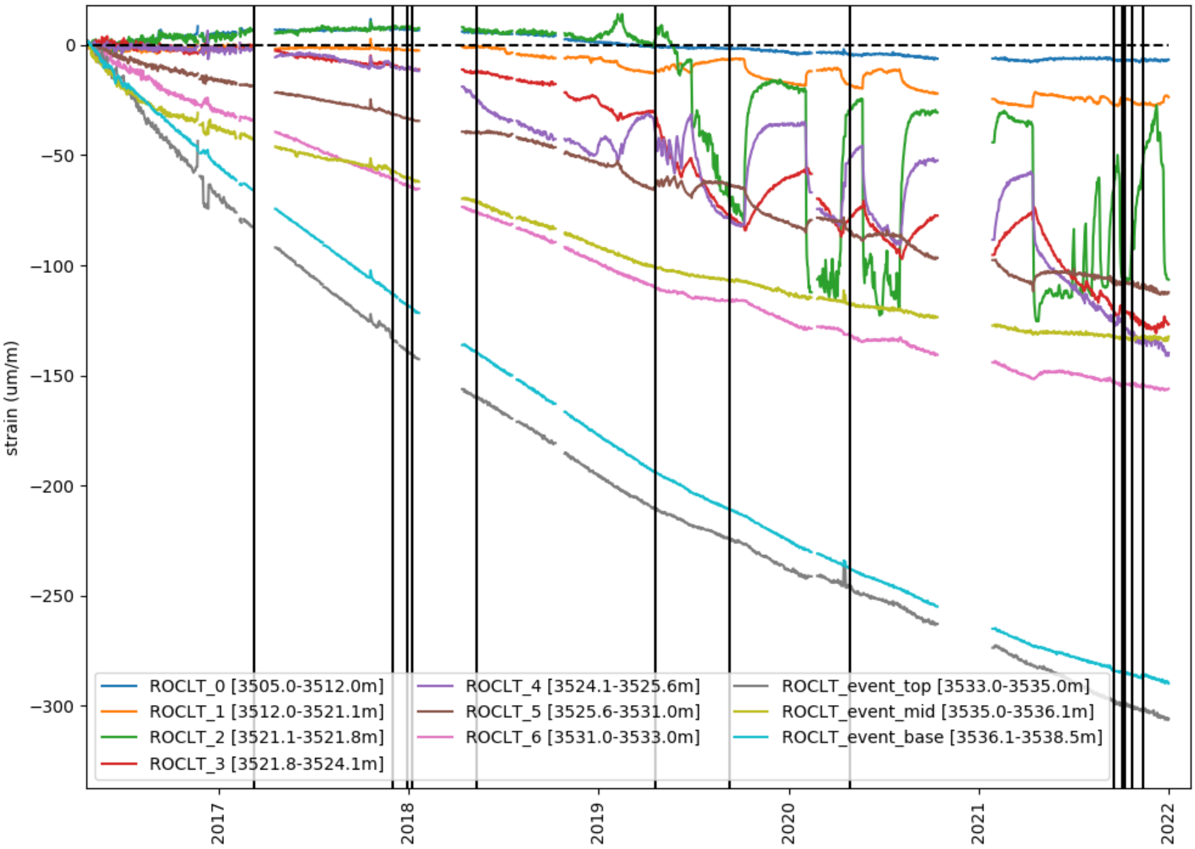

Figure 22: Strain signals over time for the subdivisions of the Ten Boer formation, with the timing of all earthquakes within 1km from Zeerijp-3A in the KNMI catalogue highlighted by black vertical lines.

REFERENCES

[1] The first year of distributed strain sensing (DSS) monitoring in the Groningen gas field irst year DSS report, NAM Feiten en Cijfers (nam.nl), 2018
[2] Analysis of and learnings from the first four years of in-situ strain data in Zeerijp-3A, NAM Feiten en Cijfers (nam.nl), 2020
[3] KNMI - Aardbevingscatalogus